A Time-Domain Simulation for Predicting the Downwind Performance of Yachts in Waves

Dougal Harris, Curtin University of Technology, Perth, Western Australia.
Giles Thomas, Curtin University of Technology, Perth, Western Australia.
Martin Renilson, Australian Maritime College, Launceston, Tasmania, Australia.

ABSTRACT

Yachts racing in many of today's high profile races, such as the America's Cup and the Volvo Ocean Race, spend much time sailing downwind in following seas. The development of a method for predicting the performance of yachts sailing downwind in waves would therefore provide a valuable design tool for racing yacht designers.

This paper describes the development of a time-domain simulation for predicting the performance of yachts sailing in irregular seas for apparent wind angles between 90 and 180 degrees. The simulation output may be used to either directly compare different designs or augment existing polar plots for the effect of a following sea.

The simulation is comprised of three main modules: the wave induced longitudinal force, the resistance force and the sail aerodynamic force. The resistance and wave force modules have been validated through semi-captive model experiments. Results from the complete simulation have been compared with those obtained from free running model experiments.

Numerical experiments on a number of hull and rig configurations have been conducted using the simulation. Results are presented with conclusions being drawn on the effect of hull form and environmental conditions on downwind performance.

NOTATION

AME	Australian Maritime Engineering
IMS	International Measurement System
SYHS	Systematic Yacht Hull Series
VPP	Velocity Prediction Program
AP	aft perpendicular (transom)
BWL	waterline beam
C_w	wave phase celerity
C_T	total resistance coefficient
D	propeller diameter
Fn	Froude number
FP	forward perpendicular
g	acceleration due to gravity
H	wave height
J	advance ratio
k	wave number ($=2\pi/\lambda$)
K_t	propeller thrust coefficient
LOA	overall length of vessel
LVDT	Linear Voltage Differential Transducer
LWL	waterline length of vessel
n	rps of propeller
n_w	number of waves in irregular spectrum
p	pressure
$-R_{fh}$	hull frictional resistance
$-R_{rh}$	hull residuary resistance
$-R_{rk}$	keel residuary resistance
$-R_t$	total resistance
$-R_{vk}$	keel viscous resistance
$-R_{vr}$	rudder viscous resistance
$-\Delta R_{fh\varphi}$	change in hull frictional resistance due to heel
$-\Delta R_{rh\varphi}$	change in hull residuary resistance due to heel
$-\Delta R_{rk\varphi}$	change in keel residuary resistance due to heel
$-\Delta R_{r\varphi\beta}$	change in residuary resistance due to heel and leeway
S(x)	submerged sectional area at distance x along hull
$S(\omega)$	irregular sea energy density spectrum
T	thrust
T_c	canoe body draft
u	yacht velocity
Va	velocity of advance
V_{aw}	apparent wind velocity
V_{awe}	effective apparent wind velocity
V_w	true wind velocity
x,y,z	Cartesian co-ordinate system, origin at AP on waterline, x forwards, y port, z vertically down
X_ξ	longitudinal wave force at position ξ in wave
x_w	distance from AP to wave crest in direction of wave propogation.
β_{awe}	effective apparent wind angle
Δ	displacement

φ	roll angle
λ	wave length
ρ	density (kg/m^3)
ω	frequency (rads/sec)
ξ	non-dimensional position in wave ($=x_w/\lambda$)
ψ	heading angle (0° head sea, 180° following sea)
ζ_w	wave amplitude

Non-dimensionalisation methods:

1. Wave induced surge force

$$X_\xi' = \frac{X_\xi}{0.5 \cdot \rho \cdot BWL \cdot H \cdot C_w^{\,2}}$$

2. Vessel velocity

$$Fn = \frac{u}{\sqrt{g \cdot LWL}}$$

3. Vessel position in wave

$$\xi = \frac{x_w}{\lambda}$$

1 INTRODUCTION

This paper discusses the development of a time domain simulation for the downwind performance prediction of yachts in waves sailing at heading angles between 90° and 180°.

Velocity Prediction Programs (VPPs) are used extensively by designers and handicap systems to predict the performance of yachts. Most current VPPs are a static force and moment balance (incorporating surge, roll, yaw and heave), often including an added resistance term for the effects of a head sea. However the traditional approach of incorporating head sea effects, as an added resistance term in the static force balance VPP, cannot be used for following seas (Kuening et. al., 1993). Since, for low encounter frequencies (invoking the quasi-steady assumption), the force on the vessel contributed by the wave is dependent only on the vessel's relative position in the wave, a time-domain simulation approach is required for the analysis of such conditions.

The development of a directly downwind longitudinal time-domain simulation for a yacht in regular following seas has previously been reported by the authors (Harris et al., 2000a). This paper reports on the further development of the code to incorporate varying yacht heading angles (directly astern through to beam seas) and diverse environmental conditions including irregular seas. The simulation may be used to either directly compare different designs in user defined conditions or to produce an adjustment to VPP output polar diagrams for the effect of a following seaway.

The longitudinal wave force on a vessel in regular following waves has been studied extensively (DuCane and Goodrich, 1962, Umeda, 1984, Thomas and Renilson, 1991, Kuening et al., 1993). The present wave force model extends to an irregular seaway, and the theory, based on the linear superposition of Froude-Krylov forces, is compared with experimental results. The effect of parametric changes in hull form, i.e. prismatic coefficient and transom shape, in the form of both theoretical predictions and towing tank results are also presented.

The resistance model uses the latest regression analysis carried out on the Delft Systematic Yacht Hull Series (Kuening and Sonnenburg, 1999). This model has been further validated by the authors through comparison with five yacht hull forms with parametric variations.

The aerodynamic force model is based on the work of Hazen (Hazen 1980), with the sail coefficients used in the model being similar to those utilised in the current IMS VPP.

The simulation has been validated using comparison with results obtained from free running model experiments in regular waves.

A series of numerical experiments on a number of hull and rig configurations has been conducted. Firstly to demonstrate the manner in which the simulation may be utilised and secondly to enable conclusions to be drawn on the effect of hull form and environmental conditions on downwind performance.

2 TIME-DOMAIN SIMULATION

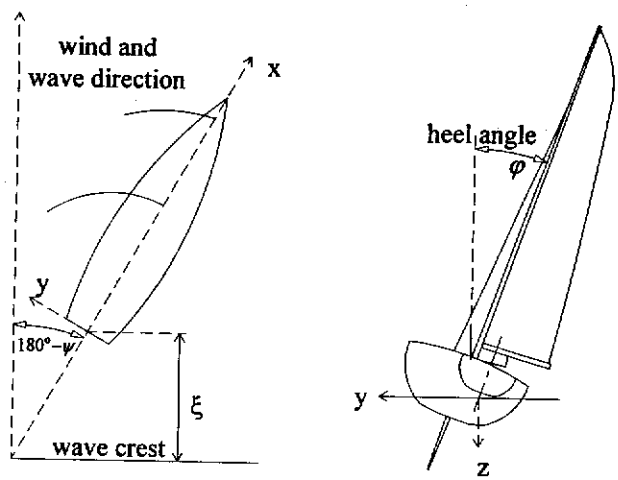

Fig. 1 Co-ordinate system

The time-domain simulation uses three input modules. Each module accounts for a force: wave force acting on the hull; aerodynamic force acting on the sail, rigging and

topsides; and the hydrodynamic resistance force acting on the submerged surface of the vessel (figure 2).

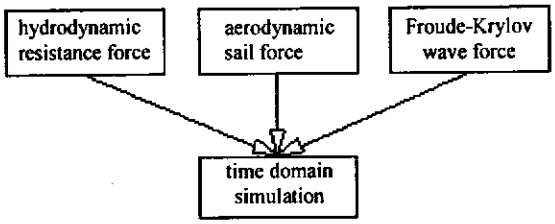

Fig. 2 Simulation modules

The simulation surge equation is represented by:

$$m\dot{u} = X_{\xi}(\xi) + R(u) + T(V_{wa}, \psi_{wa}) \qquad \textbf{Eqn. 1}$$

The wave force is a function of the vessel's position in the wave. The sail force is a function of the vessel's apparent wind velocity and direction, whilst the resistance force is a function of the vessel's velocity through the water.

Prior to the beginning of each simulation a calm water force balance (in surge, sway, heave and roll) is conducted to determine the initial velocity and the heel angle (held constant throughout the time-domain simulation). The flow chart in figure 3 demonstrates the process.

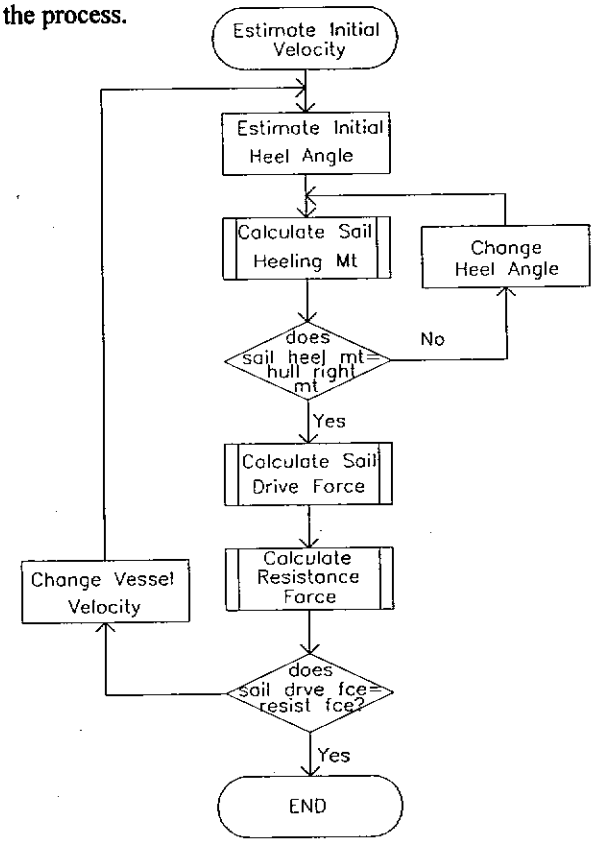

Fig. 3 Static force balance flow diagram

The simulation may be run in calm water, regular or irregular waves at angles from 180° to 90° (180° being directly downwind). The waves are always assumed to travel in the same direction as the wind. The simulation operator has a choice of three idealised sea spectra or may define the spectrum. Typical output from a single simulation run in a Pierson-Moskowitz idealised spectrum is shown in figure 4.

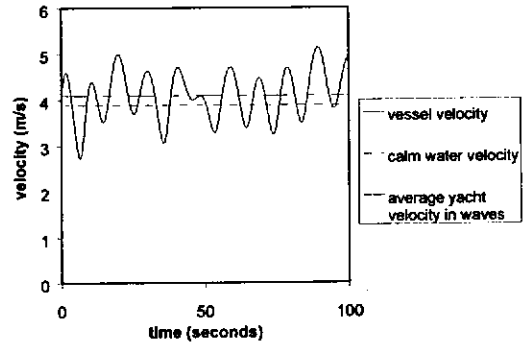

Fig.4 Typical simulation output. Hull : AME 004 Vw=15 knots, ψ=160 deg., Pierson-Moskowitz spectrum.

Due to the non-linear nature of a yacht sailing in following seas, the outcome of a simulation run in regular waves is dependent on the initial conditions. In order to investigate the effect of different initial conditions a phase plane portrait may be plotted, an example of which is shown in figure 5.

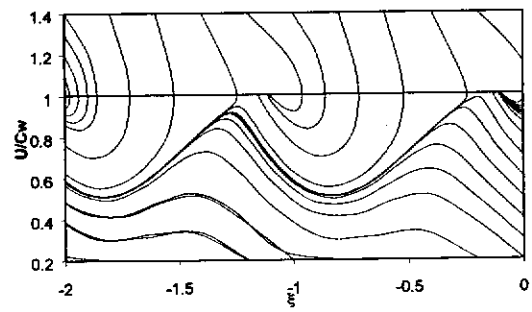

Fig. 5 Phase plane portrait. Hull : AME 004, λ=20.0m, H=1.0m, Vw=15 knots

For the single condition shown in figure 5, depending on the initial velocity and position in the wave of the yacht, it may either speed up to the wave phase velocity (u/Cw=1), the vessel is captured by the wave and is said to be 'surf-riding', or it may surge periodically as the wave overtakes the vessel. These two cases produce significantly different average velocities although they are sailing in the same environmental conditions.

The final output is a polar diagram and a typical simulation result is shown in figure 6.

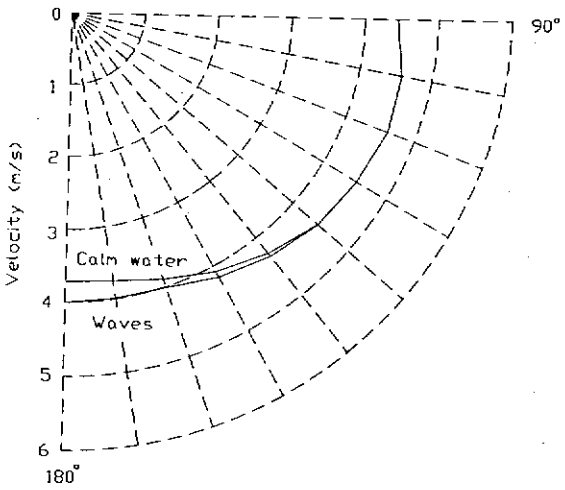

Fig. 6 Polar Plot. Hull : AME 004, Vw=7.716 m/s (15 knots), Pierson-Moskowitz irregular sea spectrum ($H_{1/3}$=1.25m).

Figure 6 demonstrates how the velocity of the vessel is influenced by the waves. The inside curve is the predicted velocity in calm water, the outside curve is the predicted velocity in the same wind conditions but in a Pierson-Moskowitz irregular sea spectrum. From 90 degrees to 120 degrees the vessel travels at approximately the same speed as in calm water, however as the true wind angle increases above 120 degrees the average velocity in following waves increases significantly over the calm water velocity.

It is possible to incorporate the time-domain simulation results into the results from any VPP. The time-domain simulation calculates the calm water velocity and the velocity in waves. From this the change in velocity due to waves at each wind angle may be calculated. This value may then be used as a 'correction' to any VPP output, accounting for the effect of a following sea. The resulting polar plot may then be used for performance prediction under a specified set of environmental conditions or over a defined race course.

2.1 Calm Water Resistance

The calm water resistance model is based on the regression polynomial fitted to results from the Delft University of Technologies systematic yacht hull series, which to date contains more than 50 hull forms (Kuening et. al. 1999). The resistance components are split into the residuary resistance on the hull and keel plus the frictional resistance of the hull, keel and rudder. Corrections are then made for each of the resistance components due to the effects of heel. Finally an induced resistance term is added due to the side force generation of the hull and appendages. The calm water resistance components may be summarised as follows:

$$R_t = R_{fh} + R_{rh} + R_{vk} + R_{vr} + R_{rk} + \Delta R_{fh\varphi} + \Delta R_{rh\varphi} + \Delta R_{rk\varphi} + \Delta R_{r\varphi\beta}$$

This regression polynomial is valid for a Froude number range of 0.1-0.6. For the Froude numbers in the range 0.6-0.75 the older regression polynomial from the Delft systematic series is used (Gerritsma et.al. 1993). At values greater than 0.75 no published data is available and a linear extrapolation is used.

2.2 Wave Force

It has been shown that the predominant force acting in surge direction in a following seaway is the Froude-Krylov force (Tuite and Renilson, 1998). Froude-Krylov wave force theory assumes a quasi-steady condition, that is the wave force experienced by the vessel is dependent only on the vessel's position in the wave and is independent of encounter frequency (for low encounter frequencies). The force arises from the undisturbed pressure field of the wave acting on the hull of the vessel. For a regular wave:

$$p = \rho g z - \rho g \zeta_w e^{-kz} \cos k(\xi + x)$$

The method, outlined below, for calculation of the Froude-Krylov force has been used with success by Umeda (1984):

$$X_\xi = -\rho g \zeta_w k \int_{x=AP}^{x=FP} e^{-kd(x)} S(x) \sin(2\pi\xi + kx) dx$$

Using the principle of linear superposition this has been extended to an irregular following seaway (Harris et. al. 2000b), composed of n regular sine waves:

$$X_\xi = -\sum_{i=1}^{n} \left(\rho g \zeta_{wi} \frac{2\pi}{\lambda_i} \int_{x=AP}^{x=FP} e^{-\frac{2\pi}{\lambda_i} d(x)} S(x) \sin(2\pi\xi + \frac{2\pi}{\lambda_i} x_w) dx \right)$$

For a vessel at a heading angle Ψ in regular waves (Umeda and Renilson, 1992):

$$X_\xi = \left(\rho g \zeta_{wi} \frac{2\pi}{\lambda_i} \int_{x=AP}^{x=FP} e^{-\frac{2\pi}{\lambda_i} d(x)} S(x) \sin\left(2\pi\xi + \frac{2\pi}{\lambda_i} x(-\cos\psi) \right) dx \right) \cdot (-\cos\psi)$$

When this formulation is applied for heading angles of 90° to 180° the wave maximum wave force varies with angle to the waves as shown in figure 7.

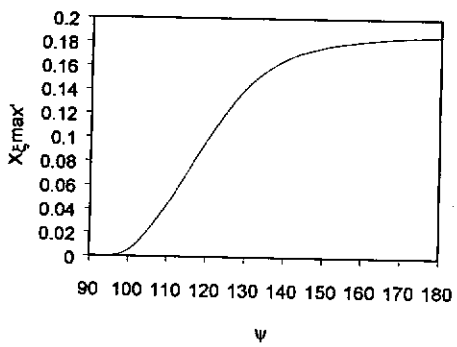

Fig. 7 Maximum longitudinal wave force as a function of heading angle, λ/LWL=1.5, H/λ=1/25, hull : AME 004.

then for an irregular sea made of n_w component sine waves:

$$X_{F-K} = -\sum_{i=1}^{n_w}\left(\rho g \zeta_{wi}\frac{2\pi}{\lambda_i}\int_{x=AP}^{x=FP} e^{-\frac{2\pi}{\lambda_i}d(x)} S(x)\sin\left(2\pi\xi + \frac{2\pi}{\lambda_i}x(-\cos\psi)\right)dx\right) \cdot(-\cos\psi)$$

2.3 Sail Force

The sail force model employed is based on work by Hazen (1980). Modifications have been made to the sail coefficients and a blanketing term introduced for the effect of the main on the spinnaker while sailing downwind. Coefficients used in the model are the same as the current IMS VPP. Coefficients are supplied at discrete apparent wind angles; therefore for other apparent wind angles a cubic spline interpolation routine is applied.

All coefficients for the sail lift and drag are for the upright condition. When the yacht heels the coefficients are not modified but the effective apparent wind velocity (V_{awe}) and direction (β_{awe}) are computed in the plane that heels with the yacht, i.e. components of the true wind are calculated in the plane normal to the mast. From geometry, neglecting leeway, it may be shown that:

$$\beta_{awe} = \beta_{aw}\cos(\varphi)$$

$$V_{awe} = \arctan\left(\frac{V_{aw}\sin(\beta_{aw})\cos(\varphi)}{V_{aw}\cos(\beta_{aw})}\right)$$

β_{awe} is then used to determine the sail coefficients and V_{awe} to determine the side and drive forces.

3 EXPERIMENTAL VALIDATION

In order to validate the time-domain simulation a number of model experiments have been conducted. Firstly semi-captive calm water tests were carried out to investigate the effect of hull form on resistance and longitudinal wave force and validate these force modules. The wave force experiments were extended to include measurements in bi-chromatic waves to validate the formulation for calculating the longitudinal wave force in an irregular following sea. The extension of the wave force formulation to angles from 90 through to 180 degrees has been validated through comparison with work conducted in the Marine Dynamics Basin of the National Research Institute of Fisheries Engineering (Umeda, 1995). Results from a set of free running experiments on a catamaran (Hannon and Renilson 2000) were utilised to validate the complete time-domain simulation.

3.1 Semi-Captive Model Experiments

The Australian Maritime Engineering Cooperative Research Centre's Systematic Yacht Hull Series was used for experimental validation of the wave force and resistance force numerical models. The series comprises 14 hull forms from which 5 were chosen to be tested in the following seas experimental program. AME 004 is the parent hull of the series (figure 8) from which parameters are varied to produce the other hulls in the series. Two hulls, AME 017 and AME 018, were built specifically for the following seas experiments. Model AME 018 has wide flat sections aft of amidships and is typical of a boat traditionally considered a fast down wind boat, while AME 017 is the opposite with narrower deeper sections aft of amidships. Other hulls in the series tested were two prismatic coefficient variation hull forms, AME 007 and AME 008. All hulls in the series were designed by the project industry participants Murray, Burns and Dovell.

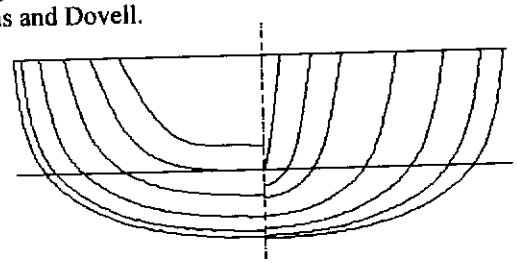

Fig. 8 Body plan parent hull of systematic series

The principal particulars of the hulls used in both towing tank and numerical experiments are given in table 1.

AME SYHS hull no.	004	007c	008b	009c	010	011c	012	013c	014c	017	018
numerical experiment	√	√	√	√	√	√	√	√	√	√	√
towing tank tested	√	√	√							√	√
overall length (m)	11.3	11.3	11.3	11.3	11.3	11.3	11.3	11.3	11.3	11.3	11.3
design LWL (m)	10	10	10	10	10	10	10	9.999	9.999	10	10
design BWL (m)	2.664	2.681	2.524	2.499	2.785	2.622	2.669	2.836	2.485	2.653	2.654
Design Tc (m)	0.417	0.423	0.416	0.343	0.486	0.363	0.48	0.39	0.446	0.416	0.418
Tested Δ (kg)	5100	5100	5100	4100	6100	5100	5100	5100	5100	5100	5100
Cp	0.536	0.513	0.554	0.534	0.535	0.533	0.536	0.535	0.535	0.536	0.534
transom area (m^2)	0.84	0.84	0.84	0.84	0.84	0.84	0.84	0.84	0.84	0.662	1.048

Table 1 Principal parameters of hulls tested

The tests were conducted in the Australian Maritime College's Ship Hydrodynamics Centre. The towing tank has a length of 60.0m, width of 3.5m and a depth of 1.5m. The maximum speed of the carriage is 4.0m/s. Semi-captive model experiments were conducted with the model free in heave and pitch while being constrained in yaw, sway, surge and roll. Heave and pitch were measured using LVDTs, while the surge and sway forces were measured using strain gauges. The vessel's position in the wave was determined using a moving capacitance wave probe.

3.11 Calm Water Resistance

The calm water resistance curve was experimentally determined with the models towed upright for a range of Froude numbers. It should be noted that no trimming moment was applied during these tests. A trimming moment is normally applied to simulate the moment

generated on the yacht from the sail driving force. However when the moment was applied to the model during subsequent following seas tests the model tended to nose dive. The removal of the trimming moment was considered as justifiable since under downwind sailing conditions all available moveable ballast (i.e. crew etc) is shifted to the stern of the vessel to try and counteract the sail trimming moment, also there will be some vertical 'lift' generated from the spinnaker which counteracts the undesired pitching moment from the mainsail.

3.12 Wave Force

The longitudinal wave force on each of the models was measured for a number of different wave conditions. The length and height of regular waves were varied to determine their effect on the wave force experienced by the model. Prior to the commencement of each run the model was lifted clear of the water to allow an undisturbed train of waves to propagate down the tank. Once the front of the packet of waves reached three quarters of the way down the tank the carriage was started. The model was then lowered into the water and when steady the 10 second data logging period was commenced. During each run the model velocity was dictated such that the encounter frequency of the wave allowed one wave to overtake the vessel during the data logging period. Work previously reported on by the authors (Harris et. al. 2000a) showed that the wave force as a function of position in wave was not significantly affected over the range of non-dimensional encounter frequencies tested ($0.2<u/C_w<1.2$). A number of tests were also conducted in bi-chromatic waves (a seaway composed of two regular waves of different frequencies) to validate the proposed numerical model for formulating the wave force in an irregular seaway (section 2.2).

3.2 Free Running Model Experiments.

To validate the use of a time-domain simulation for the prediction of motions of a vessel in following seas, results from the numerical simulation were compared with free running experimental results from tests conducted on a model catamaran (Hannon and Renilson 2000). As mentioned in section 2 the numerical model has three force components: the wave induced surge force, the hydrodynamic resistance force and the aerodynamic sail force. For comparison of the model catamaran results the sail force module was replaced with a propeller force module; this was considered acceptable as both are driving forces that are a function of the vessel's velocity. Experimental values for the resistance and wave forces, determined from semi-captive model tests, were used in the simulation. The model was free in surge, heave, roll and pitch and constrained in yaw and sway. Measurements were taken of the vessel's relative position to the carriage, carriage speed, vessel heave and pitch, propeller rpm, and the vessel's position in the wave using a moving wave probe.

4 RESULTS AND DISCUSSION

4.1 Calm water resistance

Calm water resistance experiments were conducted on all vessels ticked in row three of table 1. Experimental results compared well with the theory presented in section 2.1. A comparison of the experimental calm water results and theory for the parent hull AME 004 is presented in figure 9.

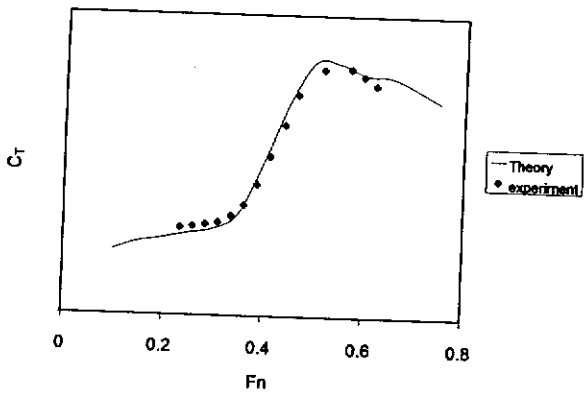

Fig. 9 Upright calm water resistance AME 004.

4.2 Wave force

The wave induced surge force was investigated in a variety of wave conditions and on a variety of yacht hull forms (Harris et. al. 2000a, 2000b). A typical regular wave force graph is shown in figure 10.

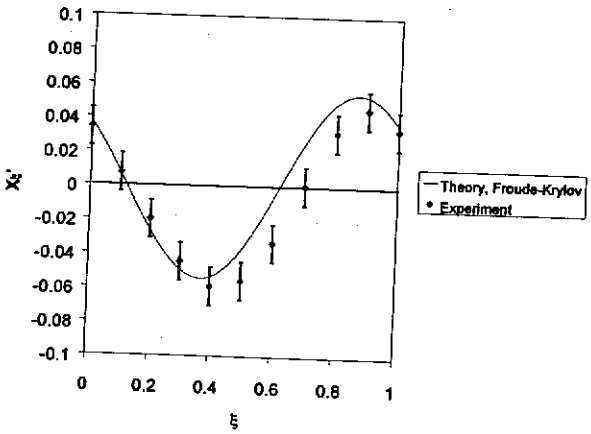

Fig. 10 Wave force vs. position in wave. AME 004, $H/\lambda=1/25$, $\lambda/LWL=3/2$.

From figure 10 it may be seen that the wave force varies periodically over the wave length. The maximum wave force is experienced at a non-dimensional position in the wave of $\xi\sim0.9$ (when the majority of the boat is on the front face of the wave) and the maximum retarding force at $\xi\sim0.4$. Error bars indicate that 95% of the experimental points lie within their span.

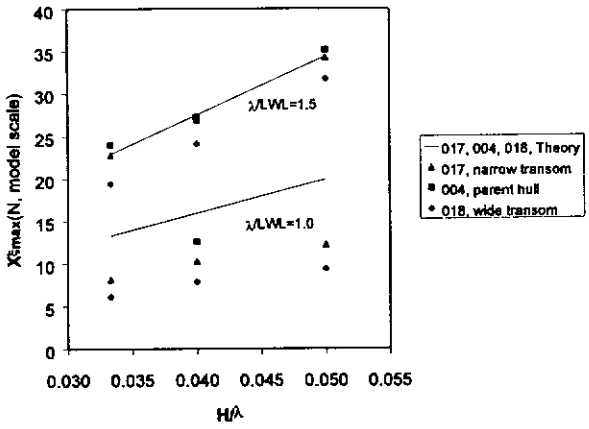

Fig. 11 Max wave force vs. wave steepness for varying transom area. LWL=2.0m.

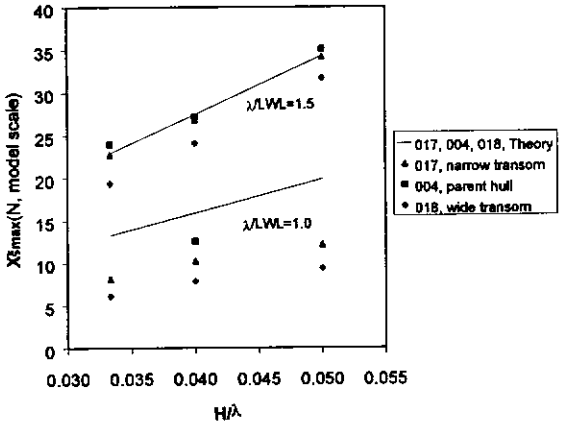

Fig. 12 Max wave force vs. wave steepness for varying prismatic coefficient

Figures 11 and 12 indicate the maximum wave force experienced by the model hulls during following seas experiments for a matrix of wave lengths and steepnesses. Model AME 017 experienced a slighter larger wave force than model AME 018 for all conditions tested. The parent hull, AME 004, experienced a wave force greater than AME 017 at λ/LWL=1.5, and a wave force between AME 018 and AME 017 for all other conditions. The wave force theory was not able to differentiate substantially between the three models. The maximum wave force increased with wave steepness and wave length. Figure 12 indicates that while the absolute values of the maximum wave force were slightly over predicted by theory the ranking of each of the hulls was generally predicted well by the theory.

To validate the proposed method for the theoretical prediction of wave force in an irregular seaway experiments were conducted in a bi-chromatic wave. A bi-chromatic wave is a seaway consisting of two waves of different frequencies. Experimental results compared well with theory. A typical plot is given in figure 13. A complete analysis of these results can be found in Harris et. al. 2000b. The experimental points are as measured in the irregular wave tests whilst the thick continuous line represents the sum of the wave forces of the two component waves, as determined by combining the forces measured in the regular wave tests. The proposed theory for determining the wave force in an irregular sea by summing the individual theoretical Froude-Krylov wave forces is also shown by the thin continuous line

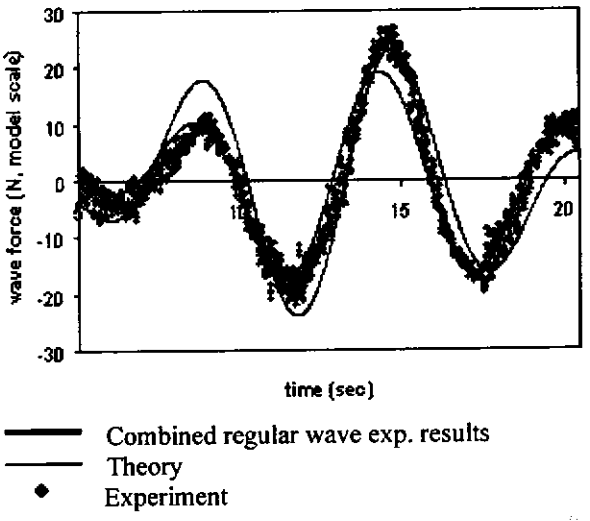

Fig. 13 Wave force vs. time, hull AME 004 in bi-chromatic wave.

In order to validate the longitudinal wave force at angles other than a directly astern following sea, Ψ=180°, model experiments would need to be conducted in an ocean basin. Unfortunately, access to such a facility was not available during this project. The work of Umeda (1995), which entailed measuring the longitudinal wave force on a semi-captive fishing vessel model at various heading angles, was therefore utilised.

Due to physical constraints the minimum heading angle obtainable was Ψ=150°. When comparing the maximum wave forces (non-dimensionalisation method outlined in notation) from experiment and theory, as a function of heading angle, figure 14 was produced:

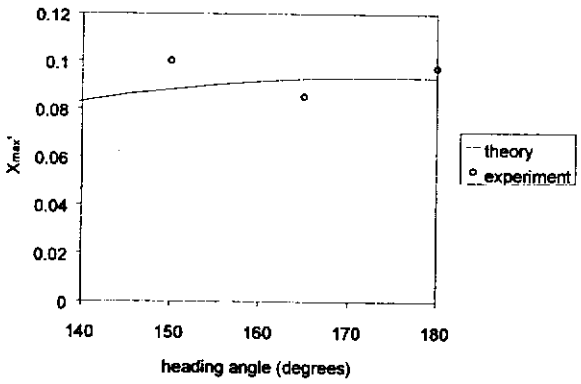

Fig. 14 Wave induced surge force on fishing trawler. H/λ=1/20, λ/LWL=1.6 (Umeda et. al .1995)

4.3 Free running model behaviour

To investigate the validity of utilising a time-domain simulation to determine the longitudinal motion of the vessel, results from the numerical simulation were compared against those obtained from free running model experiments conducted on a model catamaran in regular following seas (Hannon and Renilson 2000). The experimental data for the wave and resistance forces were used in the simulation, whilst the sail model was replaced with an experimental Kt-J curve to determine the propeller thrust. From this curve it is possible to determine the thrust generated from the propeller as a function of the velocity of advance and rpm of the propeller. Knowing the vessel's velocity of advance, Va, J may be determined:

$$J = \frac{V_a}{nD}$$

From the Kt-J curve a value for Kt may be found and the thrust developed by the propeller, T, is derived:

$$T = K_t \rho n^2 D^4$$

Principal parameters of the model catamaran used in the experiment are given in table 2.

Length overall	1.53 m
Displacement	16.03 kg
Length between perpendiculars	1.509 m
Length of waterline	1.509 m
Draft	0.066 m
Depth	0.122 m
Beam (single hull)	0.139 m
Wetted surface area	0.281 m^2
Hull separation	0.479 m
C.G. from A.P.	0.731m
LCF from A.P.	0.680 m

Table 2 Model principal parameters

Figure 15 shows that the theoretical prediction of the position of the vessel in the wave matches well with that found experimentally:

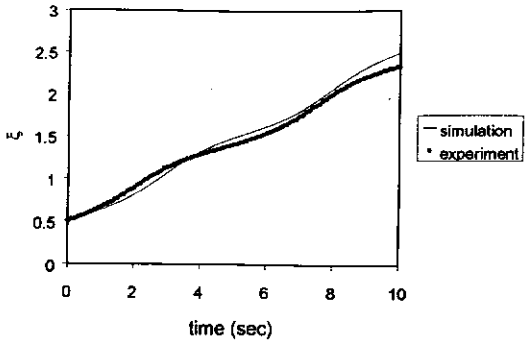

Fig. 15 Free running model experiments, non-dimensional position vs. time. λ/LWL=1.1, H/λ=0.036

Figure 16 compares the theoretical prediction of the velocity with experiment and again agreement is good. The average velocity of vessel measured during the experiment is 1.90m/s, whilst that derived by theory is 1.92m/s. This suggests that it is valid to use the simulation model, based on equation (1), to determine the longitudinal motions.

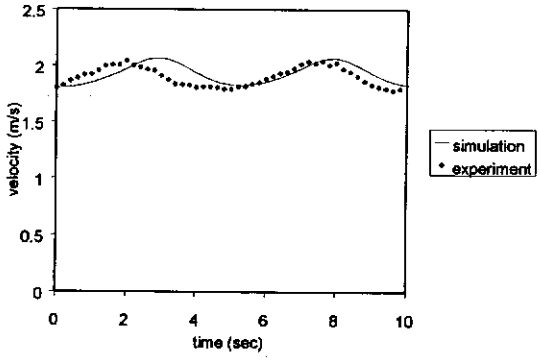

Fig. 16 Free running model experiments, velocity vs. time. λ/LWL=1.1, H/λ=0.036.

5 PARAMETRIC STUDY

The numerical simulation, using the theoretical models of force outlined in section two, was used to compare the performance of different hull forms when travelling downwind in following seas. Numerical experiments were conducted on a subset of hulls from the AME systematic yacht hull series. The aim of the series is to vary one parameter at a time from the parent hull form while keeping all other parameters as close as possible to original values. Model particulars for hulls AME 004, AME 007, AME 008, AME 017 and AME 018 are given in table 1. Simulations were run in both regular and irregular waves.

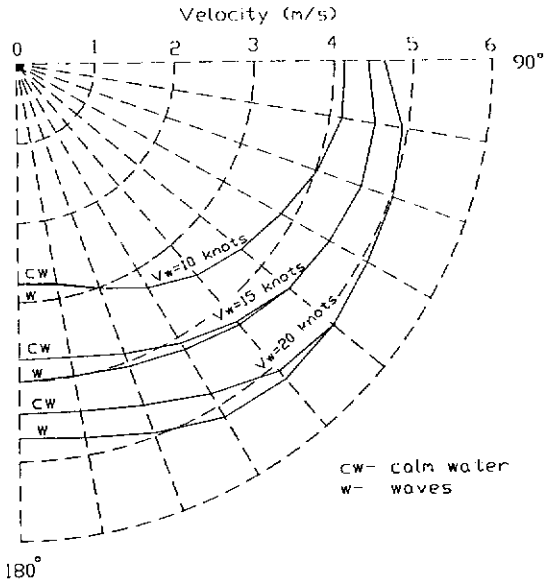

Fig. 17 Polar diagram. AME 004, Vw=10, 15, 20 knots, calm water and waves. Pierson-Moskowitz sea spectrum.

Figure 17 shows the output from simulations run in three different wind velocities for the parent hull form AME 004. The results indicate that an insignificant increase in vessel velocity, compared with calm water, is expected due to waves in 10 knots of wind. However, a significant increase in yacht speed is shown for 15 knots of wind and the largest increase of velocity in 20 knots of wind. To explain these results the method of wave definition should first be clarified. The polar diagrams produced in figure 17 were conducted in a Pierson-Moskowitz idealised sea spectrum (where V_w is the only variable required to fully define the spectrum). The Pierson-Moskowitz irregular sea spectrum for V_w=10,15 and 20 knots is given in figure 18.

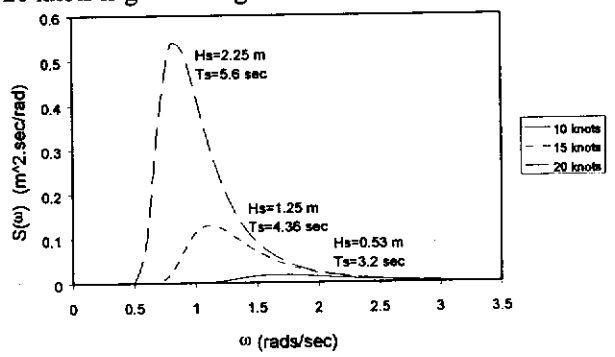

Fig. 18 Pierson-Moskowitz energy density spectra.

At Vw=10 knots the spectrum contains a relatively low amount of energy when compared to the energy in the spectrum at 20 knots. This translates into the characteristic wave height and period, and hence the wave induced force experienced by the yacht. As the wind velocity increases, the calm water velocity also increases bringing the velocity of the vessel closer to the phase velocity of the characteristic wave length. These factors explain why the difference between calm water velocity and wave velocity increases with wind speed. Another point to note is that there is very little increase in velocity due to waves at angles less than Ψ=130°. For angles 90°<Ψ<130° the longitudinal wave force is dramatically decreased when compared with Ψ=180° (see figure 7). The other factor is that the relative velocity of the wave (in the direction of the yacht's motion) to the velocity of the yacht increases significantly. The larger the relative velocity between the wave and the yacht the less time the yacht spends on the front face of the wave per surging cycle (the time taken for one wavelength to overtake/be overtaken by the yacht).

In order to compare the downwind performance of the various hull forms, the polar data was translated into expected speeds for a downwind course using the optimum VMGs. The results were then compared, using the parent hull form AME 004 as a baseline hull, to illustrate, the expected differences in time taken over a one nautical mile course directly downwind, see figure 19.

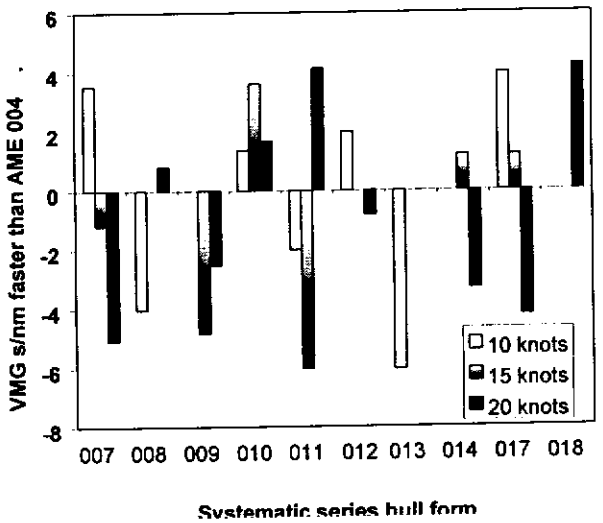

Fig. 19 VMG (downwind) comparison between hulls of systematic series for three wind velocities (10 knots, 15 knots and 20 knots)

In figure 19 a positive VMG value means seconds per nautical mile faster than the parent hull AME 004. The graph indicates that in 20 knots of wind, the wind speed for which the waves have greatest influence, AME 011 (large beam/draft rato) and AME 018 (large flat sections aft of amidships) are expected to be the fastest, whilst AME 007 (low prismatic coefficient) and AME 017 (deep narrow sections aft of amidships) are predicted to be the slowest. These results support the concept that yachts with wide flat sterns are faster when travelling downwind in waves than yachts with narrow deep sections. It is interesting to note that the trends are not consistent across

the wind speeds which suggests that any design decision should be based on running the polar data through a race modelling program, so that performance in all sailing directions (weighted according to the race course) may be taken into consideration.

6 CONCLUSIONS

A time-domain simulation for predicting the performance of yachts downwind in irregular waves, for heading angles of ψ=90° to ψ=180° , has been developed. Towing tank experiments were conducted on 5 models from the SYHS: AME 004, AME 007, AME 008, AME 017 and AME 018. Results from the calm water force module have been compared favourably with the calm water towing tank test results and theoretical longitudinal wave force results showed good agreement with tank tests in both regular and bi-chromatic waves. The change in wave force with heading angle and the motion predicted by the time-domain simulation have also been validated through comparison with experimental results. A set of numerical experiments have also been conducted on a range of hull forms.

The following conclusions may be drawn:

1. The simulation accounts successfully for the wave induced longitudinal Froude-Krylov force, the hydrodynamic resistance force and aerodynamic sail force.

2. It is valid to use a time-domain simulation to translate the component forces into a prediction of vessel motions, as validated through the free running experiments. Hence the simulation is useful for the performance of a yacht sailing downwind in waves.

3. For the conditions examined in the parametric study, the gains in speed due to waves, when utilising a Pierson-Moskowitz idealised spectrum are significant at heading angles greater than 130° and wind speeds greater than 10 knots

4. The potential of the simulation has been demonstrated through the comparison of downwind performance of a number of hull forms in a range of conditions. At the higher wind speed, and hence larger wave heights, investigated, the yacht with the flatter wider stern shape is significantly faster downwind than the yacht with the deeper narrower sections aft.

ACKNOWLEDGEMENTS

The authors would like to acknowledge the support of the Australian Maritime Engineering Cooperative Research Centre in funding the project, and industry participants Murray, Burns and Dovell for their design input and advice during the work.

REFERENCES

DU CANE, P. and GOODRICH G.J.: "The Following Sea Broaching and Surging", RINA Transactions, vol. 104, April 1962.

GERRITSMA, J., KEUNING, J.A., VERSLUIS, A.: "Sailing Yacht Performance in Calm Water and in Waves, 11th Chesapeake Sailing Yacht Symposium", Annapolis, USA, 1993.

HANNON, M.A., & RENILSON, M.R.: "Behaviour of a High Speed Catamaran in Following Seas", NAV2000, International Conference on Ship and Shipping Research, Venice, Italy, September, 2000.

HARRIS, D., THOMAS, G., RENILSON, M.R.: "Towards Predicting the Behaviour of Yachts in Following Seas", 7th International Conference on Stability of Ships and Ocean Vehicles, 2000a.

HARRIS, D., THOMAS, G., RENILSON, M.R.: "Predicting the Performance of Yachts Sailing Downwind in Irregular Following Seas", Submitted to RINA as paper for written discussion, March 2000b.

HAZEN, G.S.: "A Model of Sail Aerodynamics for Diverse Rig Types", New England Sailing Yacht Symposium, 1980.

KUENING, J.A. and SONNENBURG, U.B.: "Approximation of the Calm Water Resistance on a Sailing Yacht Based on the Delft Systematic Yacht Hull Series", 14th Chesapeake Sailing Yacht Symposium, Annapolis U.S.A. 1999.

KUENING, J.A., VAN TERWISGA, P.F., ADEGEEST, L.J.M.: "Experimental and Numerical Investigation into the Wave Exciting Forces in Large Following Seas", Yokohama Japan, FAST '93.

THOMAS, G.A. and RENILSON, M.R.: "Surf-Riding and Loss of Control of Fishing Vessels in Severe Following Seas", RINA Spring Meetings, 1991.

TUITE, A. and RENILSON, M.R.: "The Effect of Principal Design Parameters on Broaching-To of a Fishing Vessel in Following Seas", Transactions of The Royal Institution of Naval Architects, Dec 1998.

UMEDA, N.: "Resistance Variation and Surf Riding of a Fishing Boat in Following Seas", Bulletin of the National Research Institute of Fisheries Engineering, Japan, 1984.

UMEDA, N.: "Experimental study of wave forces on a ship running in quartering waves with very low encounter frequencies", Sevastianov Symposium on Ship Safety in a seaway, Kalingrad, Russia, 1995.

UMEDA, N. and RENILSON, M.R.: "Wave Forces on a Ship Running in Quartering Seas - A Simplified Calculation Method " Proceedings of the 5th International Conference on Stability of Ships and Offshore Vehicles, Melbourne, Volume 3, 1992.